J Intell Robot Syst (2016) 84:53–66
DOI 10.1007/s10846-016-0353-0

Design and Control of a Single Tilt Tri-Rotor Aerial Vehicle

Roman Czyba · Grzegorz Szafrański · Andrzej Ryś

Received: 15 December 2014 / Accepted: 8 February 2016 / Published online: 26 February 2016

Abstract The aim of this paper is to outline a design process of an attitude control system for unmanned rotorcraft. This small-scale unmanned aerial robot's concept is based on three rotors and one single tilt mechanism. Final design is consisted of mechanical construction, measurement system including navigation algorithm, as well as control structure and algorithm implementation at the last stage. It is important to underline that high attention was focused on the measurements filtering, estimation of the angular position, and in particular the practical aspects of the control implementation. Furthermore, a PID algorithm including various modified loop structures was studied. On the whole, it is worth to mention that the design, analysis and the validation tests were undertaken on the experimental aerial platform.

Keywords VTOL · Attitude control system · Navigation algorithms · Cascade control system · AHRS

R. Czyba (✉) · G. Szafrański · A. Ryś
Silesian University of Technology, 16 Akademicka St., 44-100 Gliwice, Poland
e-mail: roman.czyba@polsl.pl

G. Szafrański
e-mail: grzegorz.szafranski@polsl.pl

A. Ryś
e-mail: andrzej.rys@gmail.com

1 Introduction

Unmanned aerial vehicles (UAVs) have been a point of interest for many researchers within the last years. Number of successful missions employing UAVs resulted in enormous growth of military and commercial UAVs market. Especially vertical take-off and landing platforms (VTOLs) give a possibility to operate in a small, hard to reach and hazardous areas. Those aerial vehicles are highly maneuverable, have potential to hover and to take off as well as to fly and land in small limited area. However on the other hand VTOLs are unstable and can be difficult to supervise during the flight. Thus, control of a nonlinear plant is a problem of both practical and theoretical interest [3–7, 9, 11–13, 15–17, 20, 24, 26, 27]. It is a multidisciplinary issue with various requirements for mechanics, hardware and software.

In this paper, the proposed aerial vehicle is a platform with six degrees of freedom (DOF) which has been designed to obtain the highest level of flexibility, maneuverability and minimum power consumption. The purpose of this project was to design and assemble a vehicle consisting of three rotors, capable of stable hover flight. Although, the reduced number of actuators saves energy, at the same time it introduces the difficulty of compensating unbalanced forces acting on the vehicle. To maximize the capability of the proposed UAV, the thrust vectoring technique has been used. The main advantage of the thrust vectoring is an ability to orient the vehicle body with respect to the

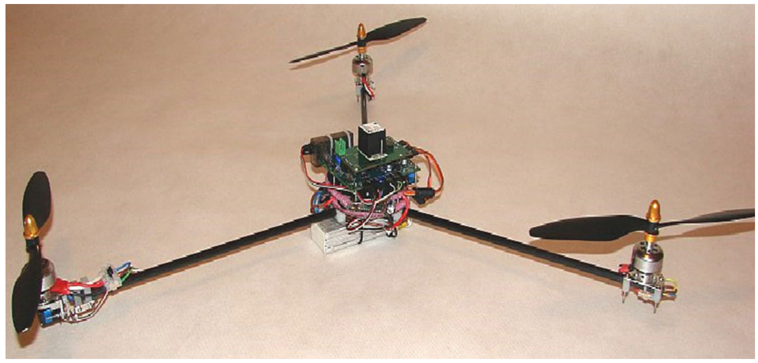

Fig. 1 Tri-rotor platform

vehicle acceleration vector. This is the basic principle of the proposed platform and in presented research tail rotor has the ability to tilt and thus control the yaw moment. Such construction is not being so popular as quadrotor [1, 3, 5, 6, 8, 14, 16, 26], although some interesting solutions can be found in the literature [2, 9, 10, 28]. In this paper a design process of the UAV, called tri-rotor, starting from concept up to flight has been presented.

The paper is organized as follows. First, a motion concept and mathematical description of constructed tri-rotor platform is introduced. During the whole paper two large research fields are investigated: measurements filtration with navigation, and control system synthesis. The first research area consisted of analysis of inertial sensors measurements, data fusion algorithms and strapdown navigation algorithms. Measurement system including data filtering was described in the Section 3. Next section presents navigation equations which are based on quaternions. Some modifications of navigation algorithm that increased robustness and performance of the Attitude and Heading Reference System (AHRS) has been also proposed. The second investigated area concerned the structure and control algorithms for attitude subsystem. In this part a general structure of a cascade control system, and investigation of a PID controllers with modified loop structure is presented. This section also includes the detailed schemes and discussion of a practical aspects of the control implementation for the under-actuated, inherently unstable system. Finally, the tests results are presented in Section 6. The conclusions are briefly discussed in the last section.

2 Principles of Mechanics and Mathematical Modelling

The platform (Fig. 1) was constructed in a shape of three-armed star, where at the end of each arm there was a fixed pitch propeller driven by a BLDC (Brushless Direct Current) motor. The major problem of rotary wing aircrafts is the torque generated by rotating massive elements. The odd number of rotors and

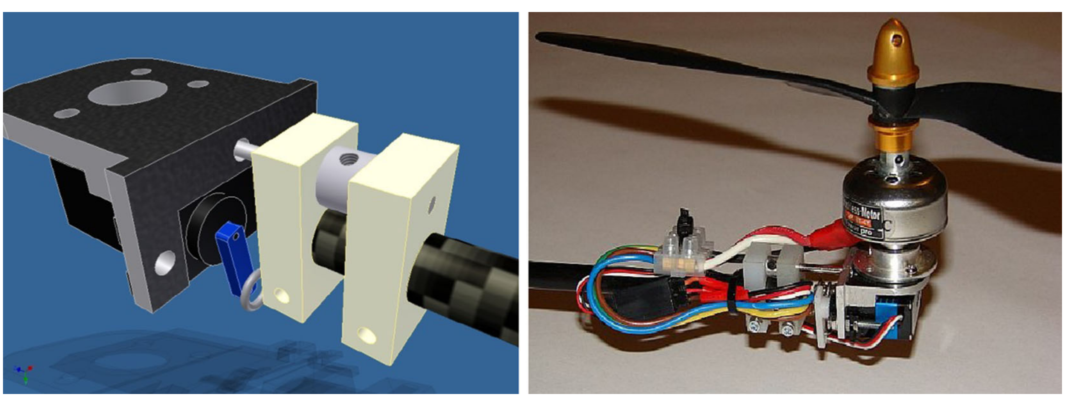

Fig. 2 Designed and assembled tilt mechanism

Table 1 Technical specification

Parameter	Value (unit)
mass	750 (g)
top diameter	73 (cm)
payload	100 (g)
flight time	∼ 15 (min)

non-symmetrical alignment brings in uncompensated forces acting on the object. This makes the modelling and control of an unsymmetrical aircraft much more complex, since the excessive forces have to be explicitly compensated by the control system. The issue that needs to be dealt with is the unbalanced torque acting on the tri-rotor caused by uneven number of motors. Alterations in the mechanical design proposed in this paper consist in introducing a tilt mechanism for one of the motors (Fig. 2). Tilt mechanism causes tilting of the motor-propeller whereby the thrust vector is generated in a desired direction. It allows to adjust the orientation of one of the motors, providing a method of compensation of excessive torque, as well as to control of the yaw angle.

General specification of tri-rotor prototype is presented in Table 1.

Motion concept of a tri-rotor is shown in the Fig. 3. If all rotors are spinning with the same angular velocity, the total torque causes rotation along yaw axis. Therefore, the motor 3 is tilted what decomposes the generated thrust into lift force and a component acting in opposite direction to the unbalanced torque. The tilt angle can be adjusted resulting in rotation along yaw axis. Roll angle changes are achieved by generating unbalanced forces by motors 1 and 2. Rotation along y-axis is caused by unequal forces produced by motor 3 and sum of motors 1 and 2.

A tri-rotor mathematical model can be divided into two subsystems (propulsion and rigid body model) as depicted in Fig. 4. It is an under-actuated system of 6 DOF and four actuators; three engines and one servomechanism. Two motors have fixed vertical position while the third one can be tilted by the servomechanism. Unlike a quadrotor, tri-rotor is not fully symmetrical object which introduces certain difficulties for the control system.

The tri-rotor flight principles can be explained by the following equations [9]:

$$\tau_\phi = (f_2 - f_1)l_1 \tag{1}$$

$$\tau_\theta = f_3 l_2 \cos\alpha - m_3 g l_2 + (f_2 + f_1) l_1 \sin\gamma – 2 m_{12} g \sin\gamma \tag{2}$$

$$\tau_\psi = f_3 l_2 \sin\alpha \tag{3}$$

where:

$\tau_\phi, \tau_\theta, \tau_\psi$	generalized moments
f_1, f_2, f_3	forces generated by motors

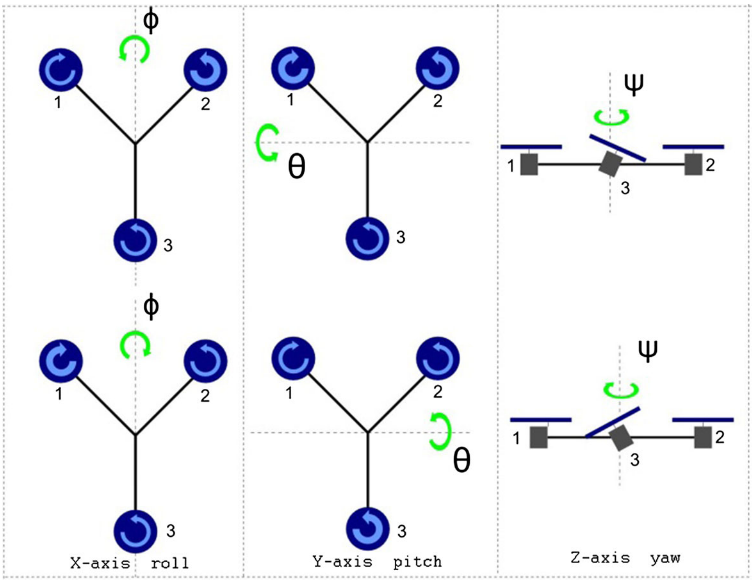

Fig. 3 Tri-rotor motion concept

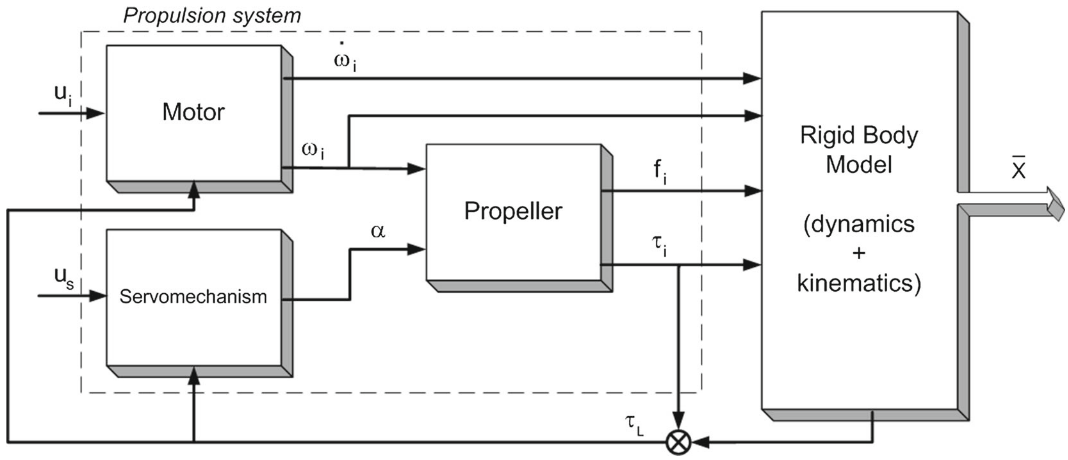

Fig. 4 Block diagram of a system dynamics

l_1	distance from the motors 1 and 2 to the x-axis
l_2	distance from the motor 3 to the center of gravity
α	tilt angle of the motor 3
γ	angle between side booms and axis y
m_{12}, m_3	motors masses

3 Measurements and Filtration System

Direct measurement of UAV attitude using inertial sensors is impossible. Therefore, an estimation process based on measurements of correlated data needs to be carried out in order to find the UAV orientation. Usually the attitude is estimated using combination of gyroscopes and accelerometers readings produced by inertial measurements units (IMUs) sometimes enhanced by other sensors like magnetometers or GPS.

In this project, Analog Devices ADIS16400 was selected as the main measurement unit. It is an integrated device containing triaxial MEMS (Micro Electro-Mechanical Systems) gyroscope, accelerometer, magnetometer and auxiliary analogue – digital converter. In the small (23 x 23 x 23 mm) and light (16g) package there are also embedded temperature and voltage sensors allowing precise biasing of readings.

Due to the MEMS sensors nature, a noise in output signal is unavoidable. Additionally, running motors generate vibrations of wide spectrum. These two sources of noise can be modeled as white noise sequence. White noise can be removed from sensors readings only by describing its statistical characteristics and applying appropriate filtering [18]. Digital linear, time-invariant (LTI) filters can be defined by a difference equation of the following form:

$$\sum_{i=1}^{M} a_i y[n-i] = \sum_{j=1}^{N} b_j x[n-j] \tag{4}$$

where:

a_i- feedback coefficients,
b_i- feed-forward coefficients.

When M=0, filter is classified as finite impulse response (FIR) and when M≠0, the filters are of infinite impulse response (IIR) type. To design a proper filter, characteristics of input signals must have been known. The measurements, sampled at 200Hz, were collected from sensors placed on tri-rotor while motors were running to provide possibly close approximation of real flight conditions. The following graph (Fig. 5) shows the PSD (Power Spectral Density) estimate of unfiltered and filtered gyroscope measurements taken in vibrating environment.

There are two main frequency intervals containing most of the noise components. Three peaks between

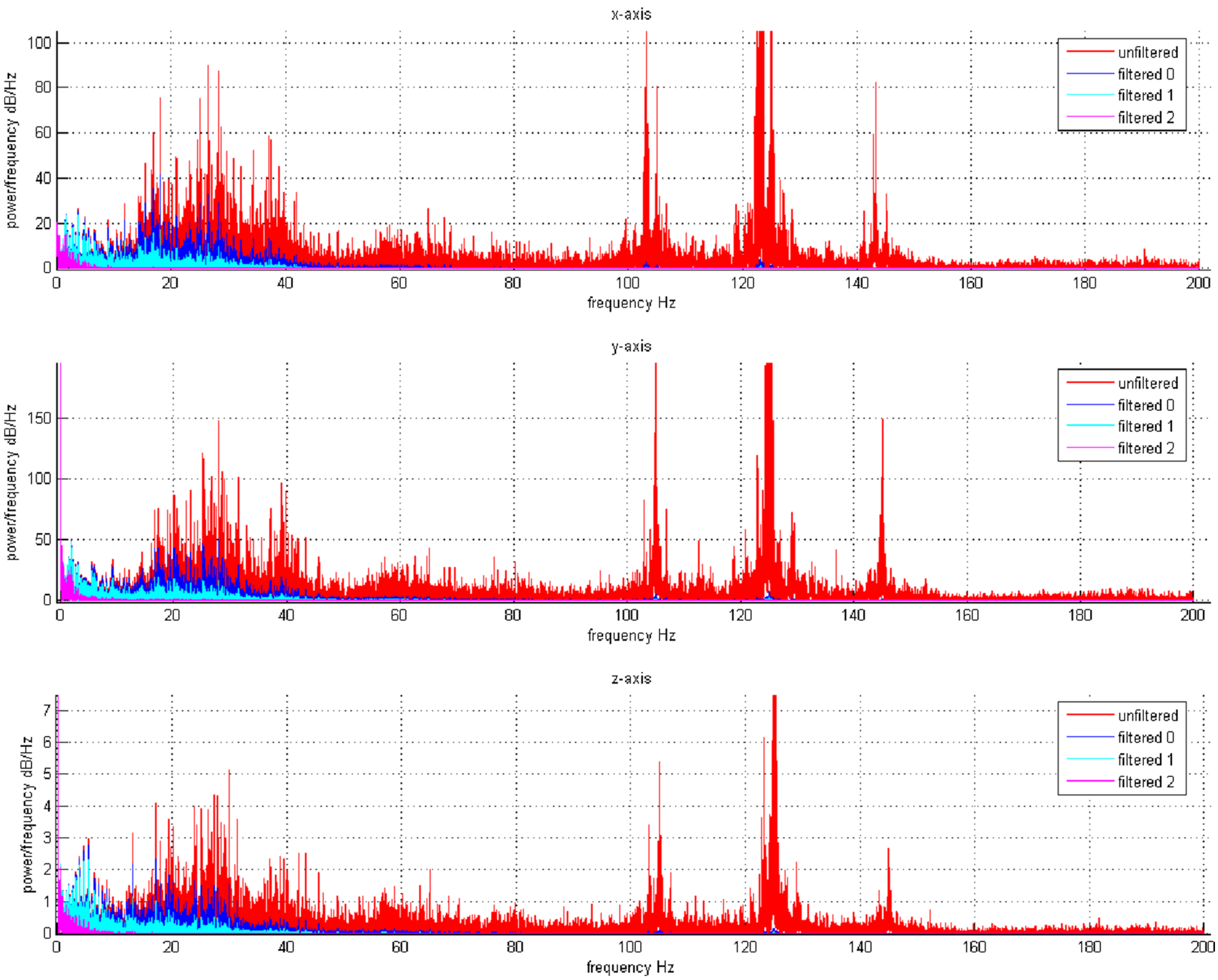

Fig. 5 PSD of unfiltered and filtered gyro measurements

100Hz and 150Hz are caused by vibrating frame due to propellers action. Exact location of these peaks is dependent on motors rotational velocity. Noise in this frequency range is not particularly harmful for the navigation because it can be very easily filtered out by a low-pass filter of relatively high cut off frequency. Noise components located between 10Hz and 50Hz have much larger negative impact on the navigation system. Filtering performed by the low-pass filter with a cut off frequency below 10Hz slows down the system significantly. On the other hand too high cut off frequency causes the navigation system collect remarkable noise, so the SNR (signal-to-noise ratio) decreases meaningfully. Tests of various filters determined that first order Butterworth IIR filters with cut-off frequency in range 10-20Hz are most suitable for this platform. These ones filter out the signal components of frequency 80-160Hz caused by rotating motors and significantly reduce low frequency noise appearing between 20Hz and 40Hz. The filters coefficients are presented in Table 2.

4 Navigation

Nowadays, inertial navigation systems are widely used on vehicles such as ships, aircraft, submarines, guided missiles and spacecrafts. The navigation algorithm defines how to process sensors readings in the navigation computer in order to obtain the current

Table 2 Filters parameters

	FILTER 0 $\omega_c = 20Hz$		FILTER 1 $\omega_c = 10Hz$		FILTER 2 $\omega_c = 5Hz$	
	a	b	a	b	a	b
1	1.0000	0.1367	1.0000	0.0730	1.0000	0.0155
2	−0.7265	0.1367	0.0730	0.0730	−0.9691	0.0155

attitude, velocity and position of the aircraft. The algorithm inputs are sensors readings with respect to the sensors frame and the output is given with respect to the reference frame.

4.1 Algorithms Overview

The simplest form of the navigation algorithm, where only gyroscopes readings are used to evaluate orientation and accelerometers to calculate velocity and position, is useful only for the high precision instruments. But for low cost sensors this approach becomes useless. Therefore, another solution capable of employing multiple sensors simultaneously to obtain an accurate attitude and position estimation is necessary. There are multiple navigation algorithms developed for low cost IMUs which try to diminish the disturbances caused by noise and drift [22]. One group of algorithms is based on complementary filters [21, 23–25] which combine high frequency gyroscopes outputs with low frequency accelerometer readings. The gyros signal is high-pass filtered while the accelerometers signal is low-pass filtered. This architecture reduces disturbances cause by high frequency noise in accelerometers readings, decreases gyros drift due to absolute accelerometer indications and maintain fast response capability having the high frequency component provided by gyros. Another group of inertial navigation systems (INS) use Kalman Filter (KF) or Extended Kalman Filter (EKF) to combine all readings provided by MARG (Magnetic, Angular Rate and Gravity) systems [19]. Although, the efficiency of KF or EKF based systems was proven in numerous publications, they require relatively powerful navigation computer. This feature disqualifies KF and EKF as navigation algorithm for this project.

4.2 Tri-Rotor Navigation Algorithm

Novel algorithm for MARG sensor, known as Magdwick algorithm [11], is an interesting approach due to a very low computational load, quaternions internal implementation and high accuracy comparable with Kalman Filter solutions. In this paper some modifications that increased robustness and performance have been proposed, and then they have been integrated into trirotor's AHRS. In the initial phase the algorithm saves the initial orientation which will be a basis for further calculation.

4.2.1 Orientation

The algorithm firstly calculates the orientation using gyroscopes readings - ${}^S_E\boldsymbol{q}_{\omega,k}$. At this stage there is no correction for drift so the error is accumulating. At the second stage it calculates the orientation using vector measurements from accelerometers and magnetometers. The original algorithm [11] uses a combination of accelerometers and magnetometers readings, however the modification introduced in this research assumes that a distinctive triple of measurements is provided for any orientation in space by both triaxial accelerometers and triaxial magnetometers. Therefore, the optimization problem from [11] has been extended to:

$$ {}^S_E\mathbf{q}_{(v,k+1)} = {}^S_E\mathbf{q}_k - \alpha_k \frac{\nabla f({}^S_E\mathbf{q}, {}^E\mathbf{g}, {}^S\mathbf{a}, {}^E\mathbf{b}, {}^S\mathbf{m})}{\|\nabla f\ ({}^S_E\mathbf{q}, {}^E\mathbf{g}, {}^S\mathbf{a}, {}^E\mathbf{b}, {}^S\mathbf{m})\|}, \quad k = 0, 1, 2, ..., n \tag{5} $$

where:

${}^S_E\mathbf{q}_{(v,k+1)}$ orientation calculated from vectors measurements,

${}^{S}_{E}\mathbf{q}_k$	last attitude estimation,
S	sensor frame,
E	Earth frame,
k	number of iteration

and

$$f({}^{S}_{E}\mathbf{q}, {}^{E}\mathbf{g}, {}^{S}\mathbf{a}, {}^{E}\mathbf{b}, {}^{S}\mathbf{m}) = \begin{bmatrix} f({}^{S}_{E}\mathbf{q}, {}^{E}\mathbf{g}, {}^{S}\mathbf{a}) \\ \hline f({}^{S}_{E}\mathbf{q}, {}^{E}\mathbf{b}, {}^{S}\mathbf{m}) \end{bmatrix} \tag{6}$$

where:

$$f({}^{S}_{E}\boldsymbol{q}, {}^{E}\boldsymbol{g}, {}^{S}\boldsymbol{a}) = \begin{bmatrix} 2g_x\left(\frac{1}{2} - q_3^2 - q_4^2\right) + 2g_y(q_1q_4 + q_2q_3) + 2g_z(q_2q_4 - q_1q_3) - a_x \\ 2g_x(q_2q_2 - q_1q_4) + 2g_y\left(\frac{1}{2} - q_2^2 - q_4^2\right) + 2g_z(q_1q_2 + q_3q_4) - a_y \\ 2g_x(q_1q_3 + q_2q_4) + 2g_y(q_3q_4 - q_1q_2) + 2g_z\left(\frac{1}{2} - q_2^2 - q_3^2\right) - a_z \end{bmatrix} \tag{7}$$

$$f({}^{S}_{E}\boldsymbol{q}, {}^{E}\boldsymbol{b}, {}^{S}\boldsymbol{m}) = \begin{bmatrix} 2b_x\left(\frac{1}{2} - q_3^2 - q_4^2\right) + 2b_y(q_1q_4 + q_2q_3) + 2b_z(q_2q_4 - q_1q_3) - m_x \\ 2b_x(q_2q_3 - q_1q_4) + 2b_y\left(\frac{1}{2} - q_2^2 - q_4^2\right) + 2b_z(q_1q_2 + q_3q_4) - m_y \\ 2b_x(q_1q_3 + q_2q_4) + 2b_y(q_3q_4 - q_1q_2) + 2b_z\left(\frac{1}{2} - q_2^2 - q_3^2\right) - m_z \end{bmatrix} \tag{8}$$

where:

- ${}^{S}\mathbf{a} = \begin{bmatrix} 0 & a_x & a_y & a_z \end{bmatrix}^T$ accelerometers normalized readings,
- ${}^{S}\mathbf{m} = \begin{bmatrix} 0 & m_x & m_y & m_z \end{bmatrix}^T$ magnetometers normalized readings,
- ${}^{S}\mathbf{g} = \begin{bmatrix} 0 & g_x & g_y & g_z \end{bmatrix}^T$ gravity field initial orientation vector,
- ${}^{S}\mathbf{b} = \begin{bmatrix} 0 & b_x & b_y & b_z \end{bmatrix}^T$ magnetic field initial orientation vector,

which claims

$$\begin{aligned} \nabla f({}^{S}_{E}\mathbf{q}, {}^{E}\mathbf{g}, {}^{S}\mathbf{a}, {}^{E}\mathbf{b}, {}^{S}\mathbf{m}) &= J^T({}^{S}_{E}\mathbf{q}, {}^{E}\mathbf{g}, {}^{E}\mathbf{b}) f({}^{S}_{E}\mathbf{q}, {}^{E}\mathbf{g}, {}^{S}\mathbf{a}, {}^{E}\mathbf{b}, {}^{S}\mathbf{m}) \\ &= \begin{cases} J^T({}^{S}_{E}\mathbf{q}, {}^{E}\mathbf{g}) f({}^{S}_{E}\mathbf{q}, {}^{E}\mathbf{g}, {}^{S}\mathbf{a}) \\ J^T({}^{S}_{E}\mathbf{q}, {}^{E}\mathbf{b}) f({}^{S}_{E}\mathbf{q}, {}^{E}\mathbf{b}, {}^{S}\mathbf{m}) \end{cases} \end{aligned} \tag{9}$$

where:

$$J^T({}^{S}_{E}\mathbf{q}, {}^{E}\mathbf{g}) = \begin{bmatrix} 2g_yq_4 - 2g_zq_3 & 2g_yq_3 + 2g_zq_4 & -4g_xq_3 + 2g_yq_2 - 2g_zq_1 & -4g_xq_4 + 2g_yq_1 + 2g_zq_2 \\ -2g_xq_4 + 2g_zq_2 & 2g_xq_3y - 4g_yq_2 + 2g_zq_1 & 2g_zq_4 + 2g_xq_2 & -4g_yq_4 + 2g_zq_3 - 2g_xq_1 \\ 2g_xq_3 - 2g_yq_2 & 2g_xq_4 - 4g_zq_2 - 2g_yq_1 & 2g_yq_4 - 4g_zq_3 + 2g_xq_1 & 2g_yq_3 + 2g_xq_2 \end{bmatrix} \tag{10}$$

and

$$J^T({}^{S}_{E}\mathbf{q}, {}^{E}\mathbf{b}) = \begin{bmatrix} 2b_yq_4 - 2b_zq_3 & 2b_yq_3 + 2b_zq_4 & -4b_xq_3 + 2b_yq_2 - 2b_zq_1 & -4b_xq_4 + 2b_yq_1 + 2b_zq_2 \\ -2b_xq_4 + 2b_zq_2 & 2b_xq_3 - 4b_yq_2 + 2b_zq_1 & 2b_zq_4 + 2b_xq_2 & -4b_yq_4 + 2b_zq_3 - 2b_xq_1 \\ 2b_xq_3 - 2b_yq_2 & 2b_xq_4 - 4b_zq_2 - 2b_yq_1 & 2b_yq_4 - 4b_zq_3 + 2b_xq_1 & 2b_yq_3 + 2b_xq_2 \end{bmatrix} \tag{11}$$

The orientations resulting from accelerometers and magnetometers readings are averaged and denoted as ${}^{S}_{E}\mathbf{q}_{v,k}$.

4.2.2 Fusion Algorithm

There are two independent sources of updates for new attitude estimation, derived from gyroscopes measurements ${}^{S}_{E}\mathbf{q}_{\omega,k}$ and from accelerometers combined with magnetometers ${}^{S}_{E}\mathbf{q}_{v,k}$. Fusion of those two estimates was performed by a complementary filter:

$${}^{S}_{E}\mathbf{q}_k = (1-\gamma){}^{S}_{E}\mathbf{q}_{(\omega,k)} + \gamma{}^{S}_{E}\mathbf{q}_{(v,k)}, \quad 0 \le \gamma \le 1 \tag{12}$$

The complementary filter has a following form:

$$ {}^S_E\dot{\mathbf{q}}_k = {}^S_E\dot{\mathbf{q}}_{(\omega,k)} - \beta\, {}^S_E\dot{\mathbf{q}}_{(v,k)} \tag{13}$$

The above Eq. 13 can be shown as:

$$ {}^S_E\dot{\mathbf{q}}_k = {}^S_E\dot{\mathbf{q}}_{(\omega,k)} - \beta\frac{\nabla f}{\|\nabla f\|} \tag{14}$$

And finally leads to:

$$ {}^S_E\mathbf{q}_k = {}^S_E\mathbf{q}_{(k-1)} + {}^S_E\dot{\mathbf{q}}_k\Delta t \tag{15}$$

The results of performance analysis of navigation algorithm are shown in the Fig. 6. Tests were performed while ADIS16400 was mounted on tri-rotor frame, motors were running and filtering was applied.

The parameter β was found during the experiments, providing fast algorithm reaction for rapid changes along with good drift correction in long run. The measure used to evaluate algorithm performance was root mean square error (RMSE). It was calculated over the interval 0-180s for each axis separately. Finally, the arithmetic mean of these values was computed and was presented in the Table 3.

The parameter β determines how big is the influence of vector measurements on the final result. For small values, the navigation performance was affected by gyros drift that could not be compensated by absolute vector measurements. For large values, the drift correction overshoots the exact solution causing the navigation algorithm operate far from the optimal solution. The tests have shown that the value of β should be close to 0,15 in order to provide highest navigation system performance.

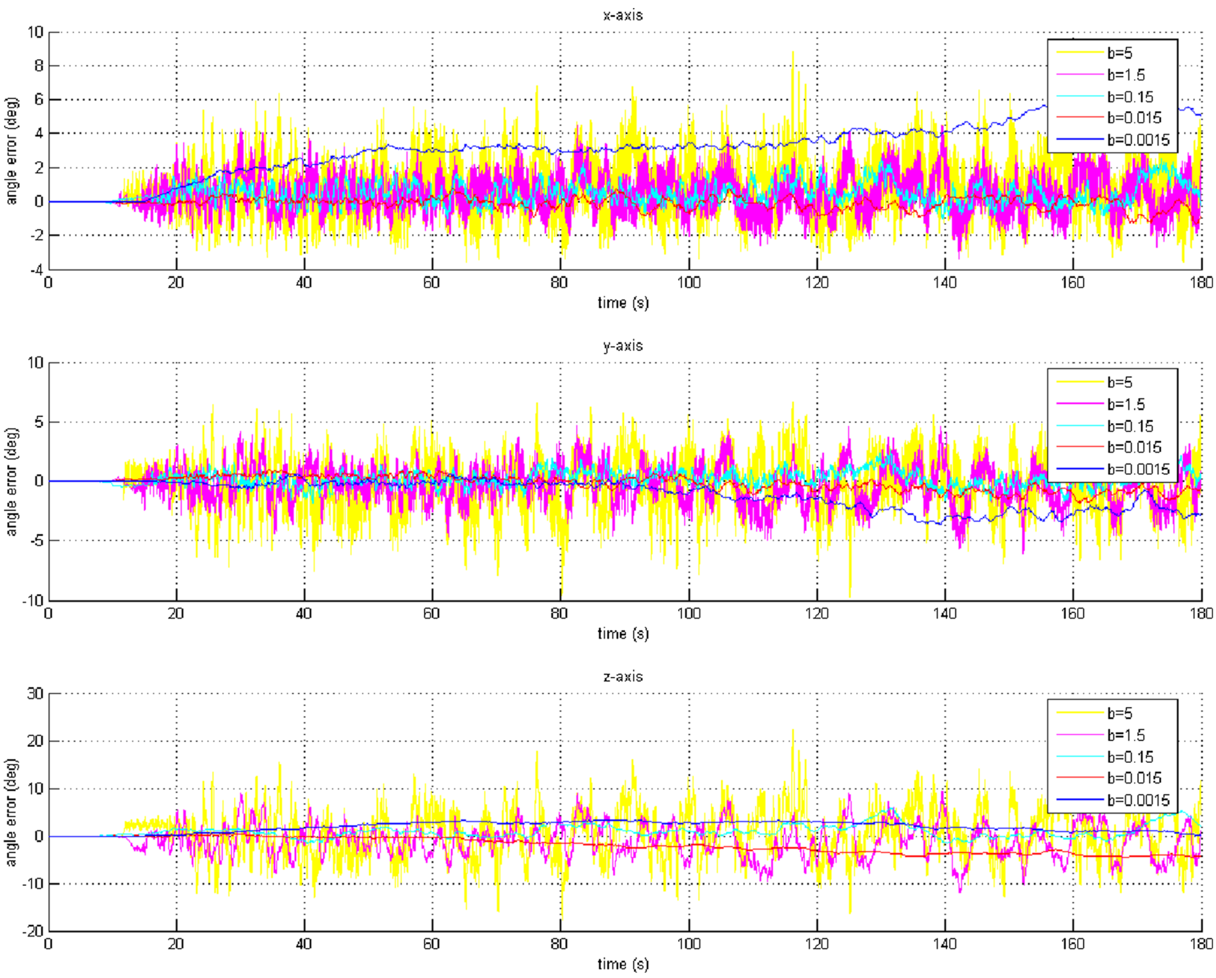

Fig. 6 Influence of parameter β on performance of navigation algorithm

Table 3 RMSE of navigation algorithm with various values of parameter β

	RMSE			
β	x-axis	y-axis	z-axis	mean
0.0015	12.5147	2.5062	4.6179	6.5463
0.015	0.1301	0.3954	6.2707	2.2654
0.15	0.6223	0.4473	2.6729	1.2475
1.5	1.3319	2.3426	12.1701	5.2815
5	3.0773	4.5904	25.1942	10.9540

5 Control System

The odd number of rotors and non-symmetrical frame brings in uncompensated forces acting on the object. This makes the control of an unsymmetrical aircraft much more complex, since the excessive forces have to be explicitly compensated by the control system.

In this paper, the control task is formulated as an angular stabilization of the tri-rotor platform, in other words as an ability to track and maintain given roll, pitch and yaw angles. General structure of the control system is shown on the Fig. 7.

System state is estimated according to the measurements obtained from a MARG sensors array. As it was already shown, ADIS16400 provides information about current angular velocity, linear acceleration and magnetic field orientation, with sample rate up to 819,2Hz. The raw data after filtration are processed by a navigation algorithm which outputs the information about current UAV orientation. It is important to note, that the dynamics of angular velocities are much faster than the attitude orientation returned by navigation algorithm. The reason is that they are measured directly by sensors, while the navigation algorithm introduces some extra dynamics. The filtration process and applied navigation algorithm have been discussed in Sections 4 and 5, respectively.

With respect to the main objective in this paper, which is the attitude stabilization, and on the basis of the research on existing control systems for UAVs, a cascade structure was chosen for realization of tri-rotor control algorithm (Fig. 7). Cascade control might be used when a process consists of two or more serial sub-processes. To apply cascade control successfully, the output of each of these processes must be measured or estimated and fulfil certain requirements. The most important requirement for a reasonable use of a cascade is a system that can be divided into two sub-systems with different dynamics. The primary controller and the primary dynamics are components of the outer loop. The inner loop is also a part of the outer loop, since the primary controller calculates the set point for the secondary controller loop. Furthermore the inner loop represents the fast dynamics, whereas the outer should be significantly slower (with respect to the inner loop).

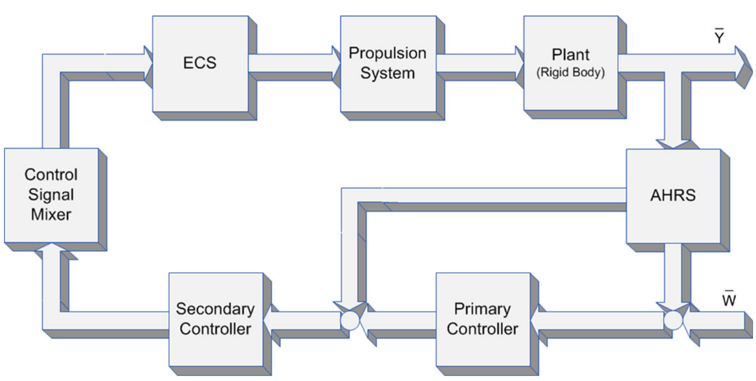

Fig. 7 General system structure

From the viewpoint of control theory, the UAV platform such as tri-rotor is nonlinear, nonstationary and multivariable. However, such platform can be controlled by PID controllers in a satisfactory manner. Practical experience shows that this kind of control can be truly valuable, mostly due to its simplicity and straightforward design. There are multiple variations of the PID controller structure [12, 13, 15]. The problem with classical PID controllers is their reaction to a step change in the reference input which produces an pulse transient in the controller action. There are two sources of the abrupt controller reaction, the proportional and derivative terms. Therefore, there are two PID controller structures that can avoid this issue. In literature exists different names [12, 15]: type B and type C; derivative-of-output controller and setpoint-on-I-only controller; PI-D and I-PD controllers. The general idea of the modified designs is to move either the derivative term or both derivative and proportional term from the main path to the feedback path. Therefore, they are not directly vulnerable to set point discontinuities, while their influence on the control reaction is preserved, since the change in set point will be still given by the remaining terms.

The control system was decoupled and in a result each of the axes has a separate control algorithm. Three controllers return separate inputs for three motors and servomechanism which need to be combined together with throttle signal in a mixer. The structure of the control signal mixer, as the output control block, is presented in the Fig. 8.

The detailed structure of the designed control system of roll angle is shown in Fig. 9. For both pitch and yaw channels the same structure has been applied.

The structure of chosen controller for the internal loop is of type B with filtered derivative [12]. The type B structure was selected in order to avoid undesired overreactions on changes in setpoint. In addition, a filter in the derivative term provides attenuation of measurement noise on control system behaviour. This loop guarantees quick reaction on disturbances in the system and easies tuning of the inherently unstable system. The outer loop, similarly to the inner one, is of type B with filtered derivative, however, there are some modifications introduced. The first modification concerns the way how the setpoint changes are applied to the system. The main concern behind it is to reduce the overshoot when the setpoint varies rapidly. One method to avoid this problem would be to use C type PID controller. Although it removes the overshoot, it might be too slow for aerial vehicle, because the desired value is being tracked only by the integral term. The method that was implemented in the tri-rotor algorithm is a low-pass filter which reduces the speed of change of the setpoint to 10deg/s which is slow enough to avoid peak reaction of proportional term, and on the other hand, fast enough to provide high UAV performance. The second algorithm

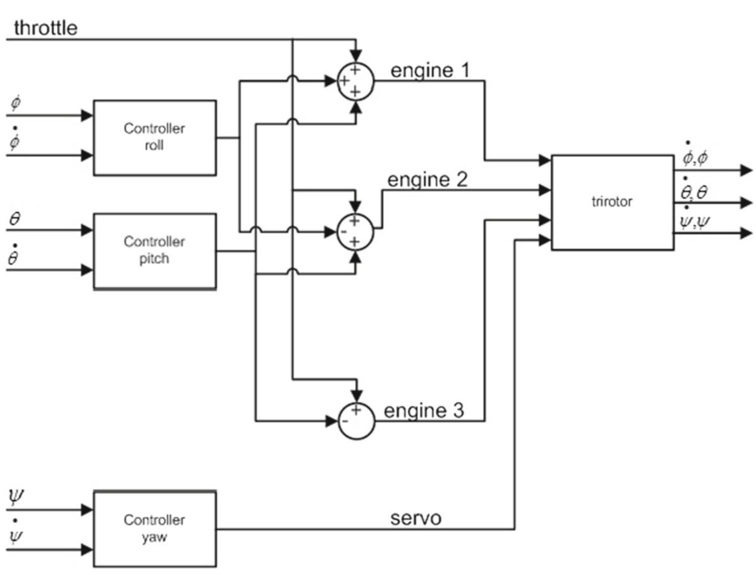

Fig. 8 Structure of the control signal mixer

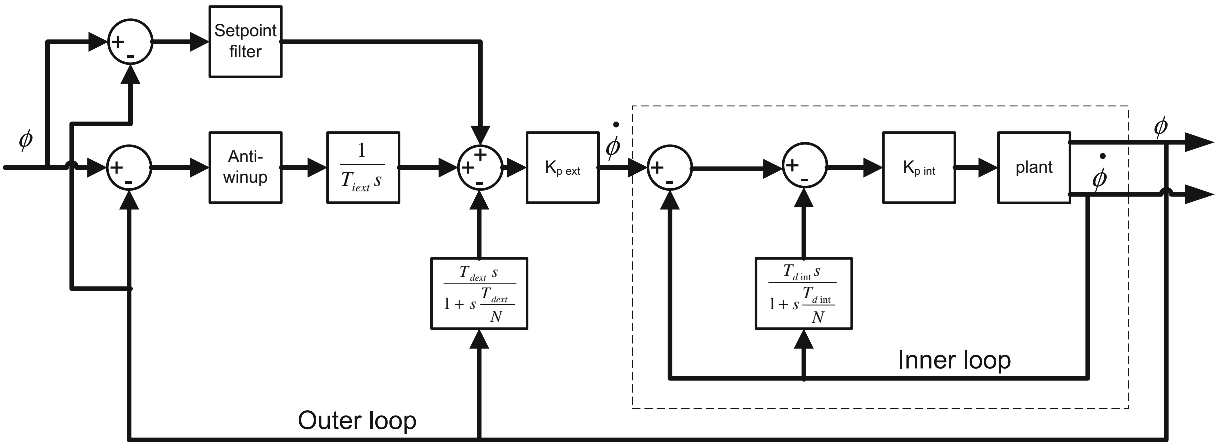

Fig. 9 Detailed structure of the control system of roll angle

enhancement is a double anti-windup protection system (Fig. 10).

It limits the maximal value of error that supplies the integral part and defines lower and upper bound for the integral term value. This method is based on comparison of the controller output with the actual actuator value. When these values are equal then the difference of them is zero and there is no influence on the algorithm. However, when the controller output falls outside the usable actuator input range, it means that the saturation occurred and the further increasing (decreasing for lower bound) of the algorithm output is undesirable. Therefore, the calculated difference is multiplied by a gain and fed back to the integral term. As a result, the integral term is supplied with lowered value or, if the gain is large enough, with a value of opposite sign, which improves an estimate of the correct state of the controller when it is not matching the real actuator input values.

The third enhancement of the algorithm is related to the derivative term of controller, because the practical implementation of the ideal PID controller is impossible. The main reason is the derivative term that causes large distortion in the control signal when high-frequency noise is present in the control loop. This problem can be significantly reduced by an additional filter in the derivative term. A common filter used to decrease the gain at higher frequencies is a first order inertia (Fig. 9). The approximation can be regarded as an ideal derivative sT_d filtered by a first order inertia with the time constant T_d/N. Thus, the approximation works as a derivative for low-frequency signal components with the gain limited to N.

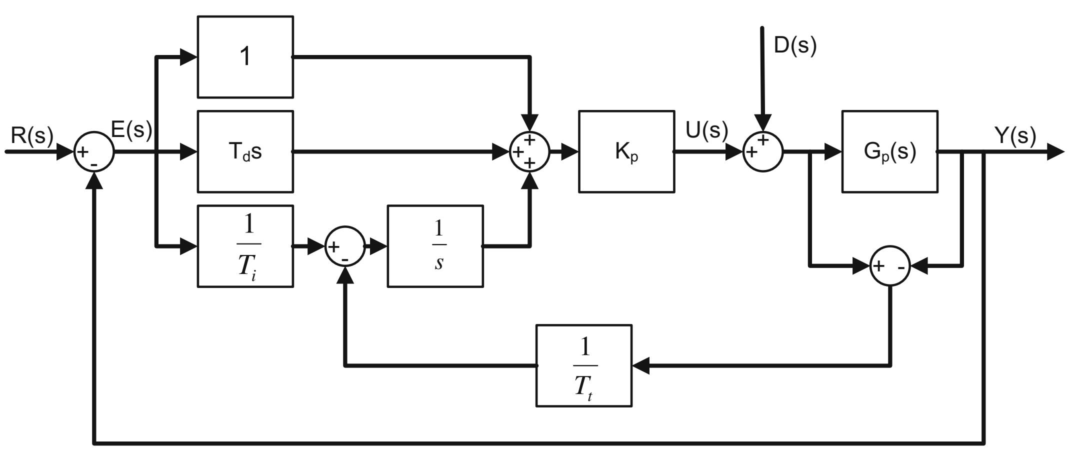

Fig. 10 PID controller with back calculation anti-windup method

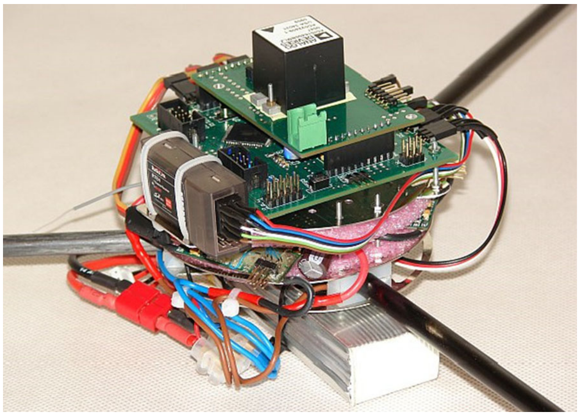

Fig. 11 Central part of the tri-rotor with dedicated electronics, AHRS, RC receiver and battery

Hardware realization of a control system in a form of an embedded microcontroller-based flight computer with AHRS is shown in Fig. 11.

6 Results

In this section, we present the results of experiments which have been conducted on the tri-rotor, to evaluate the performance of the designed attitude control system.

At first, in order to predict the performance of tri-rotor, a simulation system was developed under Matlab/Simulink platform. These integrated tools allowed to quick design, test and implement a control concept by the usage of rapid prototyping methodology. This helpful software platform was used to pre-tune controller parameters. A major role, during the angular stabilization, played the roll and pitch channels, therefore the dynamics for both angles have been assumed faster than yaw channel. The ability to maintain a given setpoint for at least 60 seconds was tested for each axis separately using a specialized stand that limited the number of degrees of freedom to one. The tuning process was conducted in accordance

Fig. 12 Tracking of the Euler angles

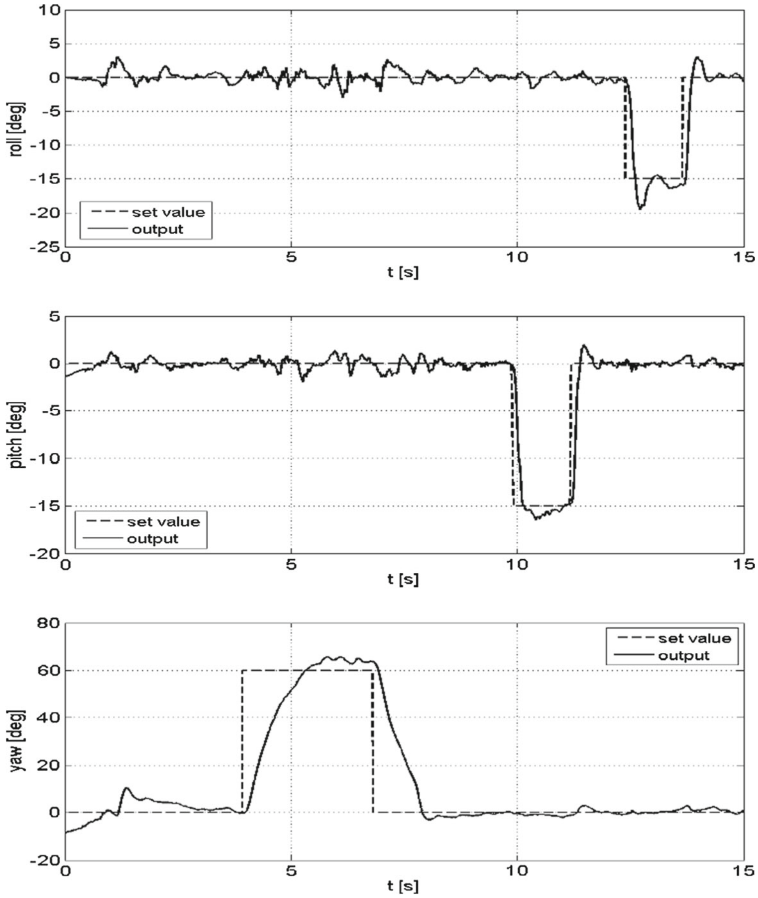

with the applicable rules for cascade systems i.e. the inner loop was tuned to have possibly high proportional and derivative gain. That setting provided good rejection of disturbances appearing in the inner loop. Secondly, the outer loop which had slower dynamics was tuned so, that the tri-rotor was able to maintain a given setpoint. Tests results were satisfactory, the tri-rotor was able to hold a given setpoint for unlimited time.

Once the tri-rotor was capable of maintaining a given, constant setpoint, it was tested against step changes in setpoints, but this time during the flight. The experiments were performed in order to examine whether all components are working properly and whether it is possible to stabilize the tri-rotor attitude. The presented maneuver consisted in transition with predefined dynamics from one steady-state angular position to another. The gains required slight modifications in order to prevent a overshoot to occur and provide damping of oscillations. Tests have proven that tri-rotor properly tracks changes of setpoints in all axes. The results are presented in the Fig. 12.

7 Conclusions

In this paper, the design process and implementation of single tilt tri-rotor UAV has been presented, including measurements filtering, navigation development, as well as control algorithm implementation at the last stage. To maximize the operational capabilities of the proposed construction the thrust vectoring technique has been used, at the conceptual stage of the design process. In this paper, high attention was drawn to the measurements filtering, estimation of the angular position, and in particular the practical aspects of the control system design. The modifications in the navigation algorithm resulted in an increase of robustness and performance of the AHRS. The designed control system consisted of an angular stabilization system for the unmanned platform. The problem of different dimensions between inputs and outputs was solved by the MIMO PID controller and control signal mixer, which allowed the control algorithm to be applied. Various PID controller structures suitable for practical implementations have also been considered. The setpoint kick in proportional and derivative terms, integral windup, and accurate approximation of derivative action were discussed. Additionally, a cascade PID control system has been introduced together with the requirements and constraints for the system to validate cascade control system application. According to results of the research on practical control systems, an appropriate system for the tri-rotor was developed in the form of a cascade PID and PD positional controllers of type B with filtered derivative terms, double integral windup protection and limited setpoint changes ratio. The navigation algorithm based on accelerometers, gyroscopes and magnetometers combined with the cascade control structure provided good stabilization during the different flight conditions. The tri-rotor was able to maintain given orientation as well as track the changes of the Euler angles. First attempts to outdoor flights were very promising and achieved results are satisfactory. Experiments results for tracking a reference signal were presented, and confirmed the effectiveness of the proposed method and theoretical expectations. The successful flight validated the previous all stages of single tilt tri-rotor UAV design.

Acknowledgments This work has been granted by the Polish Ministry of Science and Higher Education from funds for years 2014–2016.

References

1. Tayebi, A., McGilvray, S.: Attitude stabilization of a VTOL quadrotor aircraft. IEEE Trans. Control Syst. Technol. **14**(3), 562–571 (2006)
2. Chiou, J.S., Tran, H.K., Peng, S.T.: Attitude control of a single tilt Tri-rotor UAV system: dynamic modeling and each channel's nonlinear controllers design. Mathematical Problems in Engineering, vol. 2013. Hindawi Publishing Corporation (2013)
3. Nonami, K., Kendoul, F., Suzuki, S., Wang, W., Nakzawa, D. Autonomous flying robots, 1st edn. Spirnger, London (2010)
4. Raptis, I.A., Valavanis, K.P.: Linear and nonlinear control of small-scale unmanned helicopters. Springer, Dordrecht (2011)
5. Valavanis, K.P.: Advances in unmanned aerial vehicles. Springer, The Netherlands (2007)
6. Castillo, P., Lozano, R., Dzul, A.E.: Modelling and control of mini-flying machines. Springer, London (2005). ch. 3
7. Hua, M.D., Hamel, T., Morin, P., Samson, C.: Introduction to feedback control of underactuated VTOL vehicles. IEEE Control. Syst. Mag., 61–75 (2013)
8. Bristeau, P.J., Callou, F., Vissiere, D.: The Navigation and Control technology inside the AR.Drone micro UAV. Preprints of the 18th IFAC World Congress, pp. 1477–1484. Milano (2011)

9. Salazar, S., Lozano, R., Escareño, J.: Stabilization and nonlinear control for a novel trirotor mini-aircraft. In: Proceedings of the 2005 IEEE international conference on robotics and automation, pp. 2612–2617, Barcelona
10. Escareño, J., Sanchez, A., Garcia, O., Lozano, R.: Triple tilting rotor mini-UAV: modeling and embedded control of the attitude. American Control Conference, Westin Seattle Hotel, Seattle (2008)
11. Magdwick, S.O.H., Harrison, A.J.L., Vaidyanathan, R.: Estimation of IMU and MARG orientation using a gradient descent algorithm. IEEE International Conference on Rehabilitation Robotics, Switzerland (2011)
12. Visioli, A.: Practical PID control. Springer (2006)
13. Ang, K.H., Chong, G., Li, Y.: PID control system analysis, design, and technology. IEEE Trans. Control Syst. Technol. **13**(4) (2005)
14. Czyba, R.: Design of attitude control system for an UAV type-quadrotor based on dynamic contraction method, pp. 644–649. IEEE/ASME International Conference on Advanced Intelligent Mechatronics, Singapore (2009)
15. Wade, H.L.: Basic and advanced regulatory control: system design and application. ISA, USA (2004)
16. Bouabdallah, S., Noth, A., Siegwart, R., PID vs, L.Q.: control techniques applied to an indoor micro quadrotor. In: Proceedings of international conference on intelligent robots and systems, Japan (2004)
17. Ashokaraj, I., Tsourdos, A., Peter, M.G.S., White, B.A.: A robust approach to multiple sensor based navigation for an aerial robot. In: Proceedings of the 2006 IEEE/RSJ, International conference on intelligent robots and systems, pp. 3533–3538, Beijing
18. Hua, L.R., Rongqiang, L., Lei, Z.: Filtering algorithm research on MEMS gyroscope data. In: 2008 International conference on computer science and software engineering, pp. 186–189, Wuhan
19. Gary, W., Gary, B.: An introduction to the Kalman filter, July 24 (1006)
20. Batista, P., Silvestre, C., Oliviera, P., Cardeira, B.: Low-cost attitude and heading reference system: filter design and experimental evaluation. In: 2010 IEEE international conference on robotics and automation, pp. 2624–2629, USA (2010)
21. Kubelka, V., Reinstein, M.: Complementary filtering approach to orientation estimation using inertial sensors only. In: 2012 IEEE international conference on robotics and automation, pp. 599–605, USA (2012)
22. Lee, J.K., Park, E.J., Robinovitch, S.N.: Estimation of attitude and external acceleration using inertial sensor measurement during various dynamic conditions. IEEE Trans. Instrum. Meas. **61**(8), 2262–2273 (2012)
23. Mahony, R., Hamel, T., Pflimlin, J.M.: Nonlinear complementary filters on the special orthogonal group. IEEE Trans. Autom. Control **5**, 53 (2008)
24. Tsend, S.P., Li, W.L., Sheng, C.Y., Hsu, J.W., Chen, C.S.: Motion and attitude estimation using inertial measurements with complementary filter. In: Proceedings of 2011 8th asian control conference, Taiwan (2011)
25. Yoo, T.S., Hong, S.K., Yoon, H.M., Park, S.: Gain-scheduled complementary filter design for a MEMS based attitude and heading reference system. Sensors **11**, 3816–3830 (2011)
26. Alzu'bi, H., Sababha, B., Alkhatib, B.: Model-based control of a fully autonomous quadrotor UAV. In: AIAA Infotech@Aerospace (I@A) Conference, Paper AIAA-2013-5136, USA (2013)
27. Lin, F., Ang, K.Z.Y., Wang, F., Chen, B.M., Lee, T.H., Yang, B., Dong, M., Dong, X., Cui, J., Hang, S.K., Wang, B., Luo, D., Zhao, S., Yin, M., Li, K., Peng, K., Cai, G.: Development of an unmanned coaxial rotorcraft for the DARPA UAVForge Challenge. Unmanned Systems, vol.1, no. 2, World Scientific Publishing Company, pp. 211–245 (2013)
28. Mohamed, M.K., Lanzon, A.: Design and control of novel Tri-rotor UAV, 304–309

Roman Czyba is a head of laboratory "Embedded Control Systems", an assistant professor in the Faculty of Automatic Control, Electronics and Computer Science, Silesian University of Technology. His area of research are Control Systems in Unmanned Aerial Vehicles, Nonlinear Control Systems, Robust Controllers, Embedded Control Systems, Rapid Prototyping, Real-Time and Hardware-in-the-Loop Simulation, Modeling and Simulation of Control Systems.

Grzegorz Szafrański received the M.S. degree in Automation and Robotics in 2008. He is currently working toward the Ph.D. degree in automation and robotics at Silesian University of Technology. His areas of research are data fusion algorithms, system identification and control of unmanned vehicles. He also design an electronics based on embedded systems for the modern control applications.

Andrzej Ryś is a graduate student of the Faculty of Automatic Control, Electronics and Computer Science, Silesian University of Technology. His areas of research are Unmanned Aerial Vehicles, Embedded Controllers, Automotive Systems.